ELSEVIER

Carbohydrate Polymers 43 (2000) 63–73

Carbohydrate Polymers

www.elsevier.com/locate/carbpol

Size characterisation of modified celluloses in various solvents using flow FFF-MALS and MB-MALS

B. Wittgren*,[1], K.-G. Wahlund

Division of Technical Analytical Chemistry, Centre for Chemistry and Chemical Engineering, Lund University, P.O. Box 124, S-221 00 Lund, Sweden

Accepted 24 November 1999

Abstract

The size characterisation of modified celluloses is a necessary, but also complex, task that often requires use of different methods. In this paper, two different size characterisation methods were used to obtain molar mass and size information of three hydroxypropylmethyl cellulose (HPMC) samples in four different solvents. The two methods employed were the combination of flow field-flow fractionation and multi-angle light scattering (MALS) as well as sole utilisation of the MALS instrument itself performed in the so-called micro-batch mode (MB-MALS). The influence of the different solvents, on the obtained molar mass and size for the HPMC-samples was found to be pronounced. For example, the molar mass obtained for the high molar mass HPMC 10000 increased from 310,000 up to 650,000 g/mol when the solvent was shifted from a 50% methanol–salt mixture into 1 mM NaCl. Also the radius of gyration was clearly affected by the change in solvent. Theses changes were compared with values of the second virial coefficient, A_2, obtained from MB-MALS. Furthermore, both techniques were able to identify clear differences in solution behaviour between the HPMC-samples, which were delivered by two different manufacturers. It was concluded that the two methods gave comparable results and complement each other well in the size analysis of these complex polymers.

Keywords: Modified cellulose; Size characterisation; Flow field-flow characterisation method; Multi-angle light scattering method

1. Introduction

Cellulose derivatives belong to a group of polysaccharides of importance in various pharmaceutical applications. In such applications, the solution behaviour of these polymers is an essential issue that needs to be thoroughly characterised. One general parameter to study then is the size of the polymer, usually expressed in terms of molar mass and molar mass distribution. Lately, static light scattering measurements, using efficient high effect laser sources and computer-aided calculations, are being applied in order to obtain absolute determinations of molar mass also in practice (Kratochvil, 1987; Wyatt, 1993). One way to use this technique is to measure the scattered light at many different angles and at different concentrations of the polymer in order to construct the grid-like Zimm plots (Kratochvil, 1987). From these plots, information about the characteristics, i.e. the molar mass, the radius of gyration and the second virial coefficient of the studied polymer in solution, can be obtained, as illustrated in Fig. 1. This approach has the disadvantage that only averages of the parameters mentioned are determined. For the often very broadly distributed celluloses, the distribution of molar mass and size is of particular interest (Harding, Varum, Stokke & Smidsrod, 1991) and could preferably be determined by an online combination of a multi-angle light scattering detector with a size separation technique, e.g. size exclusion chromatography (SEC) or field-flow fractionation (FFF). SEC is the traditional technique used for size separation of polymers and for determination of molar mass distribution. When it comes to polysaccharides, however, such determinations are often complicated due to non-ideal interactions between these polymers and the column material, commonly leading to sample adsorption, shear degradation or exclusion (Harding et al., 1991; Nilsson, Sundelöf & Porsch, 1995). One separation technique that can be regarded as a useful alternative to SEC for the characterisation of polymers is flow field-flow fractionation (flow FFF), a method of separation, particularly well suited to fractionate and characterise large macromolecules and particles of varying origin (Giddings, 1993). The method is universal and can deal with a very wide size range of the sample, from 1 nm up to 50 μm, of

* Corresponding author.

[1] Present address: Substance Analysis, AstraZeneca R&D, 431 83 Mölndal, Sweden.

0144-8617/00/$ - see front matter
PII: S0144-8617(99)00193-9

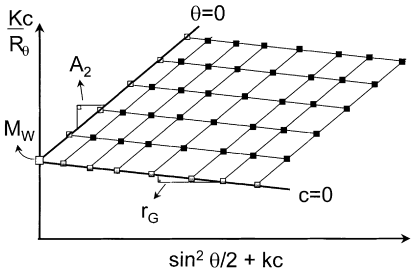

Fig. 1. The principle of Zimm plots. The scattering intensity is measured at different concentrations (c) of the polymer and at different angles (θ) and plotted versus $\sin^2(\theta/2) + kc$ where k is a constant of arbitrary value. Extrapolations to both $c = 0$ and $\theta = 0$ are then performed (heavy lines). The second virial coefficient, A_2, can be determined from the slope of the line where $\theta = 0$ whereas the radius of gyration, r_G, is obtained from the slope of the line where the concentration is extrapolated to zero. The intercept provides the molar mass.

major advantage in the characterisation of large and polydisperse polysaccharides.

Previous work has indicated the potential of flow FFF, connected to a multi-angle light scattering (MALS) detector, for the characterisation of some different water-soluble polymers (Adolphi & Kulicke, 1997; Roessner & Kulicke, 1994; Wittgren & Wahlund, 1997a). One of these polymers was hydroxypropylmethyl cellulose (HPMC), which belongs to a group of modified celluloses used as excipients in drug formulations (Wittgren & Wahlund, 1997b). In this study, flow FFF-MALS turned out to provide reasonable information regarding the molar mass, the radius of gyration and the conformation of HPMC in a certain solvent. This study is now continued emphasising the influence of different solvents as well. Furthermore, as a comparison and complement to the flow FFF-MALS measurements, the MALS instrument alone is used in the micro-batch mode (MB-MALS) to provide Zimm plots and thereby determining the weight average molar mass, the z-average radius of gyration and the second virial coefficient of the HPMC polymers in the different solvents.

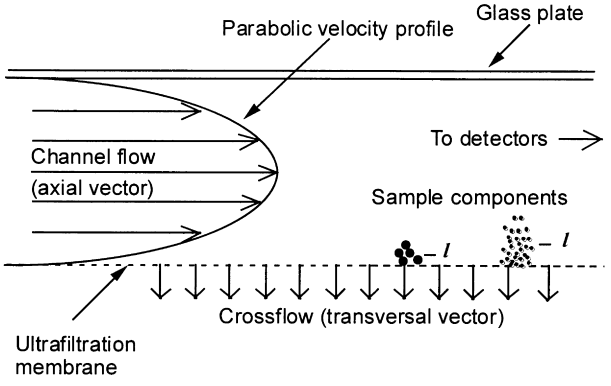

Fig. 2. The asymmetrical flow FFF channel. The carrier flow with a parabolic velocity profile is pumped along the channel. The sample components are influenced by both the channel flow (the axial vector) which transports them in the axial direction to the detector and the cross flow (the transverse vector), which presses them towards the membrane. The separation in time is dependent on position of the centre of mass, l, which in turn is determined by the diffusion coefficient of each component.

1.1. Static light scattering

Static light scattering is a well-known, absolute technique for measurements of molar mass (Kratochvil, 1987; Wyatt, 1993; Zimm, 1945), which can be obtained from a light scattering experiment using low angles of measurement by the relationship

$$\frac{Kc}{R_\theta} = \frac{1}{M_w} + 2A_2c \tag{1}$$

where the constant K is given by

$$K = \frac{4\pi^2\bar{n}_0^2(\mathrm{d}n/\mathrm{d}c)^2}{\lambda_0^4 N_A} \tag{2}$$

in which c is the solute concentration, R_θ is the excess Rayleigh factor, θ the scattering angle, A_2 the second virial coefficient, $\bar{n}_0$ the refractive index of the solvent, ($\mathrm{d}n/\mathrm{d}c$) the refractive index increment of the polymer in solution, λ_0 the wavelength of the light and N_A the Avogadro number.

For large particles, where the radial axis of the particle is larger than 5% of the wavelength, a special form factor $P(\theta)$ is introduced (Kratochvil, 1987)

$$P(\theta)^{-1} = 1 + \frac{16\pi^2\langle r_G^2\rangle}{3\lambda_0^2}\sin^2(\theta/2) \tag{3}$$

where $\langle r_G^2\rangle^{1/2}$ is the root mean square radius or more commonly the radius of gyration.

The form factor changes Eq. (1) into

$$\frac{Kc}{R_\theta} = \frac{1}{P(\theta)M_w} + 2A_2c \tag{4}$$

By measurements of the scattering intensity at different angles and concentrations, an MALS instrument can provide information about molar mass and radii averages as well as estimations of the second virial coefficient. In practice, this can be done by using the micro-batch procedure, i.e. by injecting different concentrations of the polymer solution directly into the MALS detector. The molar mass, the radius of gyration and the second virial coefficient are then determined from Zimm plots as shown in Fig. 1.

1.2. Flow FFF-MALS

FFF is a separation technique suitable for large macromolecules and particles in the broad size range of 1 nm to 50 μm. It was first presented by Giddings more than 30 years ago. The basic principle of this technique is that the separation takes place in a thin flat channel (Fig. 2), through which a liquid flow that carries the sample components is pumped (Giddings, 1973; 1993). This axial flow has a parabolic velocity profile with the highest speed in the channel centre. Perpendicular to this flow a force of various origins

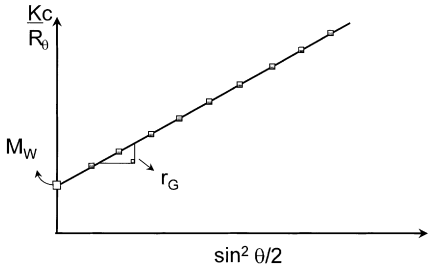

Fig. 3. The principle of the Debye plot using the Zimm method (Eq. (5)). Contrary to the Zimm plot, the Debye plot only utilises information from different angles. The radius of gyration, r_G, is obtained from the slope and the molar mass from the intercept. The Debye plot requires dilute solutions, i.e. the term A_2c in Eq. (4) should be small.

is applied. In the case of flow FFF, this force constitutes of a secondary flow, the so-called crossflow (Fig. 2). Consequently, the sample components will be forced towards one of the channel walls. However, this transport is counter-acted by the Brownian motion, so that the position of the components, i.e. the centre of mass of the zone, above the channel wall, will be strictly based on the diffusion coefficient of the macromolecule and the crossflow rate applied. Due to the parabolic profile of the axial flow, this vertical position determines the transport time of the macromolecule through the channel. It is thus possible to calculate the diffusion coefficient and the hydrodynamic size, directly from the retention time. For a more complete description of the theory of the asymmetrical variant of flow FFF used in this paper, the reader is referred to previous publications (Litzén, 1993; Litzén & Wahlund, 1991; Wahlund & Giddings, 1987; Wittgren, Wahlund, Derand & Wesslén, 1996).

Although diffusion coefficients are determined by flow FFF, for macromolecules it is often desirable to transform this parameter into the more desired property molar mass. This is, however, not conveniently done for most polymers since it requires knowledge of some properties of the sample in the particular solvent. The possibility of combining the flow FFF system with an online static light scattering detector has therefore greatly improved the capability of determining the molar mass and its distribution (Roessner & Kulicke, 1994; Wittgren & Wahlund, 1997a). If the MALS instrument is connected to a separation system such as size exclusion chromatography or field-flow fractionation equipped with a concentration sensitive detector, refractive index or photometric, it is possible to measure the scattering intensity and the sample concentration in each small slice *i* of the fractionated sample. In this approach, the A_2 term in Eq. (4) will be neglected since the dilution in the separation process is considerable leading to a very low concentration in each slice.

$$\frac{Kc_i}{R_{\theta_i}} = \left[\frac{1}{P(\theta)_i}\right]\left[\frac{1}{M_i}\right] \quad (5)$$

If the left hand side in Eq. (5) is plotted versus $\sin^2(\theta/2)$ (the so-called Debye plot) one obtains, for every slice in the fractionated peak, the molar mass and radius of gyration according to Fig. 3. Thus, with these joint techniques, information regarding distributions of molar mass and radius are obtained as well as different averages. In addition, the weight average molar mass and the number average molar mass, M_n, gives the polydispersity index, M_w/M_n. From the flow FFF retention time, it is also possible to obtain information about the hydrodynamic size, which makes the combination of these two methods a competent team in the field of polymer characterisation.

Table 1
The (d*n*/d*c*)-values for the HPMC-samples determined in the different solvents used

Sample/ Solvent	50% methanol[a] 50% 10 mM NaCl[b]	10% methanol[a] 90% 10 mM NaCl[b]	1 mM NaCl[b]	100 mM NaCl[b]
HPMC 50	0.132	0.136	0.139	0.134
HPMC 4000	0.120	0.129	0.133	0.133
HPMC 10000	0.119	0.127	0.132	0.135

[a] HPLC-grade, Merck, Darmstadt, Germany.
[b] P.a., Merck, Darmstadt, Germany.

2. Experimental

2.1. Materials

Three HPMC samples of different viscosity grades and from different manufacturers were analysed: HPMC 2910, viscosity grade 10000 cps (“HPMC 10000”) (Methocel E10M, Dow Chemicals, Midland, USA), HPMC 2910 4000 cps (“HPMC 4000”) (Methocel E4M, Dow Chemicals, Midland, USA) and HPMC 2910 50 cps (“HPMC 50”) (Metolose 60SH-50, Shin-Etsu Chem Co, Japan). The solid material (water content 3% determined by thermogravimetric analysis) was dispersed in a hot carrier solvent at 65°C that was cooled in a refrigerator overnight so as to dissolve the polymer. The four different solvents are presented in Table 1. They were filtered using a 0.2 μm regenerated cellulose filter SM 116 (Sartorius AG, Goettingen, Germany). The temperature in the carrier solvent was approximately 24°C.

2.2. Flow FFF-MALS

The flow FFF-MALS system used (Fig. 4) was identical to the one thoroughly described previously by Wittgren and Wahlund (1997b), and the reader is referred to this paper for further details. The separation channel had an asymmetrical design and a thickness of 0.0119 cm. The ultrafiltration membrane, NADIR UF-10c (Hoechst AG, Wiesbaden, Germany) having a cutoff of 10,000 g/mol, was made of regenerated cellulose. The injector (Rheodyne 9125 syringe injector, Rheodyne Inc, Cotati, CA) was equipped with a

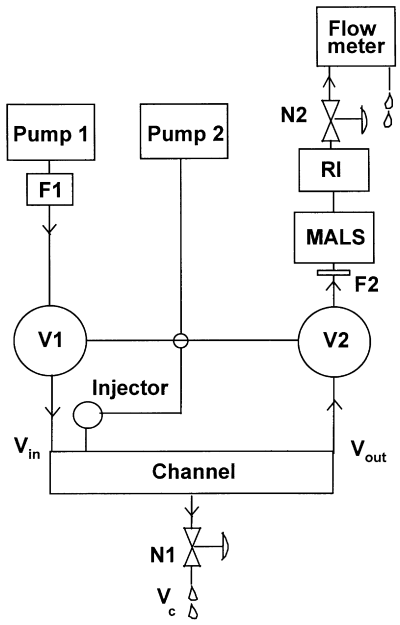

Fig. 4. The flow FFF-MALS system during the elution phase. The two detectors, MALS and RI, are connected to the channel outlet via the inline filter F2 (pore size 0.45 μm). The carrier flow from pump 1 is purified by the inline filter F1 of a pore size of 0.02 μm. The crossflow rate versus the outlet flowrate is adjusted by needle valves, N1 and N2, the outlet flowrate is measured continuously by a flow meter.

20 μl loop. The inlet flowrate (V_{in}) was varied between 1.25 and 3.0 ml/min at a constant outlet flowrate (V_{out}) at about 1.0 ml/min thus giving a crossflow rate (V_c) in the interval of 0.25–2.0 ml/min. The sample concentration injected was varied between 0.1 and 1.2% (w/w). The multi-angle light scattering instrument employed was a DAWN DSP detector (Wyatt Technology, Santa Barbara, CA), connected online directly after the flow FFF channel. A filter holder (Precolumn Filter A315 Upchurch Scientific Inc, Oakharbor, WA) equipped with a filter (regenerated cellulose filter paper SM 116 Sartorius AG, Goettingen, Germany) of pore size 0.45 μm was placed in between the channel and

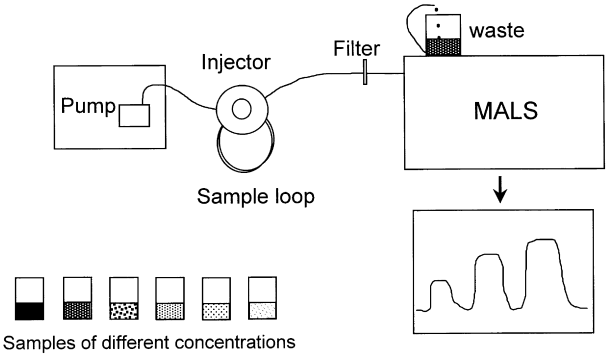

Fig. 5. The MB-MALS setup. At least six different concentrations of the dissolved polymer are injected via the injector to the MALS detector. The sample loop volume and the pump flow should be optimised as to achieve MALS responses having a plateau region.

the detector to improve the light scattering signal. Simultaneous concentration detection was performed using an Optilab DSP interferometric refractometer (Wyatt Technology, Santa Barbara, CA). Both detectors used a wavelength of 633 nm. Filtered toluene (HPLC-grade from Merck, Darmstadt, Germany) was used for calibration of the scattering intensity and NaCl (Suprapur, Merck, Darmstadt, Germany) for calibration of the refractive index. The detectors at different angles in the MALS instrument were normalised to the 90° detector using pullulan P-50 (Shodex STANDARD P-82, Showa Denko, Tokyo, Japan) and bovine serum albumin (BSA) (Sigma Chemical Co, St Louis, MO) at a flowrate through the detectors of 1 ml/min. BSA was also used to determine the interconnection volume between the detectors to 0.137 ml. The flowrate through the detectors, V_{out}, was constantly held at about 1 ml/min. Molar mass and radius data were obtained from Debye plots using the so called Zimm method, i.e. by plotting the Kc/R_θ ratio against $\sin^2(\theta/2)$ (Eq. (5)), for at least 11 different angles.

2.3. Micro-batch MALS

In the MB measurements, the MALS detector described above was connected directly after the sample injector, i.e. the sample was directly injected in to the detector without any prior separation. The MB-MALS system is illustrated in Fig. 5. The injector loop volume was then increased to 1000 μl to ensure a plateau region, of constant scattering intensity for each injection. The flow from the LC-pump (Kontron HPLC pumps 420 Kontron Instruments, Zurich, Switzerland) was continuously held at a rate of 0.5 ml/min. The filter holder described above, equipped with a 0.45 μm filter, was placed online after the injector to reduce the noise in the light scattering signal. This was especially important for the low molar mass HPMC 50. Six different concentrations of each sample in all four solvents were carefully prepared and injected. The concentration range was between 0.05 and 0.5 mg/ml. The data obtained were then evaluated using ASTRA® software (ASTRA for Windows 4.2, Wyatt Technology, Santa Barbara, CA).

2.4. The dn/dc measurements

The value of the refractive index increment (d*n*/d*c*) is essential, to know if the molar mass is to be calculated (Eq. (2)). It was determined here in each solvent by direct injection of six different concentrations of each sample into the refractometer. The data obtained from these experiments were evaluated by the DNDC5 software (Wyatt Technology, Santa Barbara, CA). The results are seen in Table 1.

3. Results

The complex solution behaviour of cellulose derivatives makes it troublesome to obtain reliable data regarding their

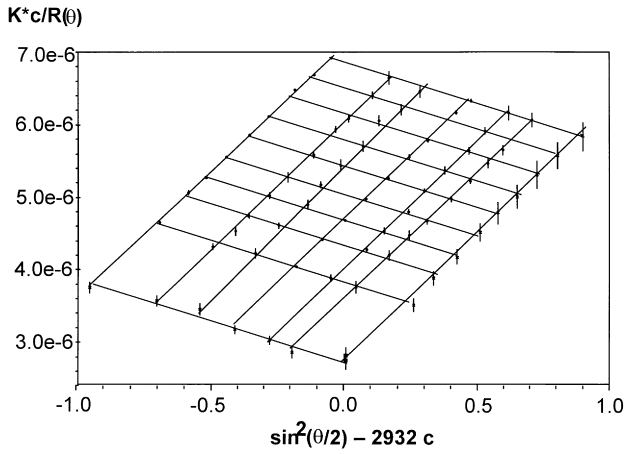

Fig. 6. The Zimm plot obtained for HPMC 10000 in 50% methanol/50% 10 mM NaCl using six concentrations and nine angles. The molar mass is 386,000 g/mol, the radius of gyration is 66 nm and the second virial coefficient is 0.0025 mol/ml g^2 for this particular run.

size and conformation using existing analytical techniques. It is clear that the choice of solvent is crucial in order to provoke a suitable hydrophobic–hydrophilic environment for the polymer so as to be able to balance the polymer–polymer and the polymer–solvent interactions. This is of special importance in SEC analyses in order to avoid interactions with the packing material. In flow FFF, however, the open channel design reduces these problems but still the membrane interactions, chain entanglement and overloading effects cannot be excluded. Some of these effects are as well closely connected with the polymer solution behaviour. For HPMC, a mixture of methanol, salt and water (50% MeOH, 50% 10 mM NaCl), has previously turned out to be favourable in the sense that in this medium interactions with the SEC material was minimised (Nilsson et al., 1995). Also in our previous flow FFF-MALS study of HPMC, this particular methanol-containing mixture was used. In the present work, however, we have chosen to study the effects of different concentrations of methanol, water and NaCl on the obtained molar mass and size of the three different HPMC samples. The solvent quality can be estimated from the micro-batch light scattering measurements, where the second virial coefficient A_2 is obtained. The possibility of also obtaining A_2 values is of special interest since this parameter could be used in the evaluation of changes in conformation, e.g. by aggregation, suggested by changes in observed molar mass and size.

The quality of the light scattering data in micro-batch mode depends greatly on the signal-to-noise ratio during data collection. Since there is no separation procedure prior to detection that can remove or separate particles and dust from the true sample components, it is essential to insert a filter between the injector and MALS. This would be especially important for the low molar mass polymers giving a weak MALS response. It is also important to use a sufficiently large injection loop and a suitable flow rate to ensure that a constant MALS response is generated over sufficient time. With necessary precautions taken, Zimm plots of as good quality as the one illustrated in Fig. 6 for HPMC 10000 were obtained. Results from the MB-MALS experiments are summarised in Table 2. The flow FFF experiments were performed at different flow rates and polymer concentrations in a way following the experimental procedures developed previously (Wittgren & Wahlund, 1997b) and the data presented in Table 3 represents the preferred experimental conditions concerning flow rates and sample concentration.

3.1. Methanol–salt–water mixtures

For the 50% methanol/50% 10 mM NaCl solution, there is a relatively good agreement between the molar mass from MB-MALS and from flow FFF-MALS. According to flow FFF-MALS, HPMC 10000 has a weight-average molar mass around 300,000 g/mol compared with 225,000 g/mol for HPMC 4000 and 132,000 g/mol for the low viscosity sample HPMC 50 (Wittgren & Wahlund, 1997b). In addition, HPMC 50 appears to be much more polydisperse than the other two samples but since they are not manufactured by the same company a difference in manufacturing process and thus polydispersity may be expected. With MB-MALS however, the molar mass for the two high viscosity samples was higher, 341,000 and 383,000 g/mol for HPMC 4000 and HPMC 10000, respectively, whereas the molar mass obtained for HPMC 50, 122,000 g/mol, deviates less from the flow FFF-MALS measurements. The difference in radii seems to be less pronounced for HPMC 4000 and HPMC 10000 but is relatively high for HPMC 50. The radius of gyration obtained was rather high compared to the molar mass, especially for HPMC 50 which had a lower M_w/r_{Gz}-ratio than the others, and this indicates a more extended conformation. For HPMC 50, the expanded conformation was further supported by the high A_2 values observed, indicating a good solvent contact. It should be mentioned that the light scattering response is rather weak for HPMC 50 in comparison to HPMC 4000 and HPMC 10000. Thus, the obtained results for this polymer, from both MB-MALS and flow FFF-MALS, are the least reliable. Improved quality of the light scattering response may be achieved by using a filter having a smaller pore size, i.e. 0.2 μm, which on the other hand may affect the detection of the high molar mass components in the broad distribution of HPMC 50.

According to both methods, a decrease in the methanol content to 10% provoked changes in observed molar mass and size. The molar mass obtained from flow FFF-MALS increased 10–15% for HPMC 4000 and HPMC 10000, in analogy with the MB-MALS results. Still, the molar mass from MB-MALS is significantly higher for both HPMC 4000 and HPMC 10000. On the contrary, for HPMC 50, a decrease in molar mass was detected using flow FFF-MALS whereas an increase was recorded with MB-MALS. The

Table 2
The molar mass M_w, the radius of gyration r_{Gz} and the second virial coefficient A_2 obtained from MB-MALS. The data presented are based on at least three different experiments

	HPMC 50				HPMC 4000				HPMC 10000			
	M_w (g/mol)	r_{Gz} (nm)	M_w/r_{Gz} (10^3 g/(mol nm))	A_2 (10^3 mol/(ml g^2))	M_w (g/mol)	r_{Gz} (nm)	M_w/r_{Gz} (10^3 g/(mol nm)	A_2 (10^3 mol/(ml g^2))	M_w (g/mol)	r_{Gz} (nm)	M_w/r_{Gz} (10^3 g/(mol nm))	A_2 (10^3 mol/(ml g^2))
50% MeOH 50% 10 mM NaCl	122,000	50	2.4	7.8	341,000	67	5.1	3.2	382,000	66	5.8	2.6
10% MeOH 90% 10 mM NaCl	138,000	53	2.6	8.7	375,000	69	5.4	2.6	462,000	74	6.2	1.6
1 mM NaCl	135,000	56	2.4	11	417,000	69	6.0	0.7	667,000	81	8.2	1.1
100 mM NaCl	133,000	63	2.1	12	363,000	62	5.9	1	506,000	74	6.8	1.5

Table 3
The weight average molar mass M_w, the polydispersity index M_w/M_n, the *z*-average radius of gyration r_{Gz}, the M_w/r_{Gz}-ratio and the recovery obtained from flow FFF-MALS experiments in the different solvents. The data presented are based on at least three different experiments. The M_w/r_{Gz}-ratio is included since it is sensitive to changes in conformation

Sample	HPMC 50					HPMC 4000					HPMC 10000				
Solvent	M_w (g/mol)	M_w/M_n	r_{Gz} (nm)	M_w/r_{Gz} (10^3 g/(mol nm))	Rec. (%)	M_w (g/mol)	M_w/M_n	r_{Gz} (nm)	M_w/r_{Gz} (10^3 g/(mol nm))	Rec. (%)	M_w (g/mol)	M_w/M_n	r_{Gz} (nm)	M_w/r_{Gz} (10^3 g/mol nm))	Rec. (%)
50% MeOH	132,000	3.7	58	2.1	85	225,000	1.91	68	3.3	83	309,000	1.93	73	4.1	90
10% MeOH 90% 10 mM NaCl	128,000	3.4	60	2.1	80	226,000	1.90	69	3.9	74	344,000	1.7	81	4.4	79
1 mM NaCl	135,000	3.2	67	2.0	72	444,000	2.8	84	5.3	57	635,000	1.8	90	7.5	60
100 mM NaCl	121,000	3.0	75	1.9	82	314,000	3.0	70	4.5	76	439,000	3.4	90	4.4	68

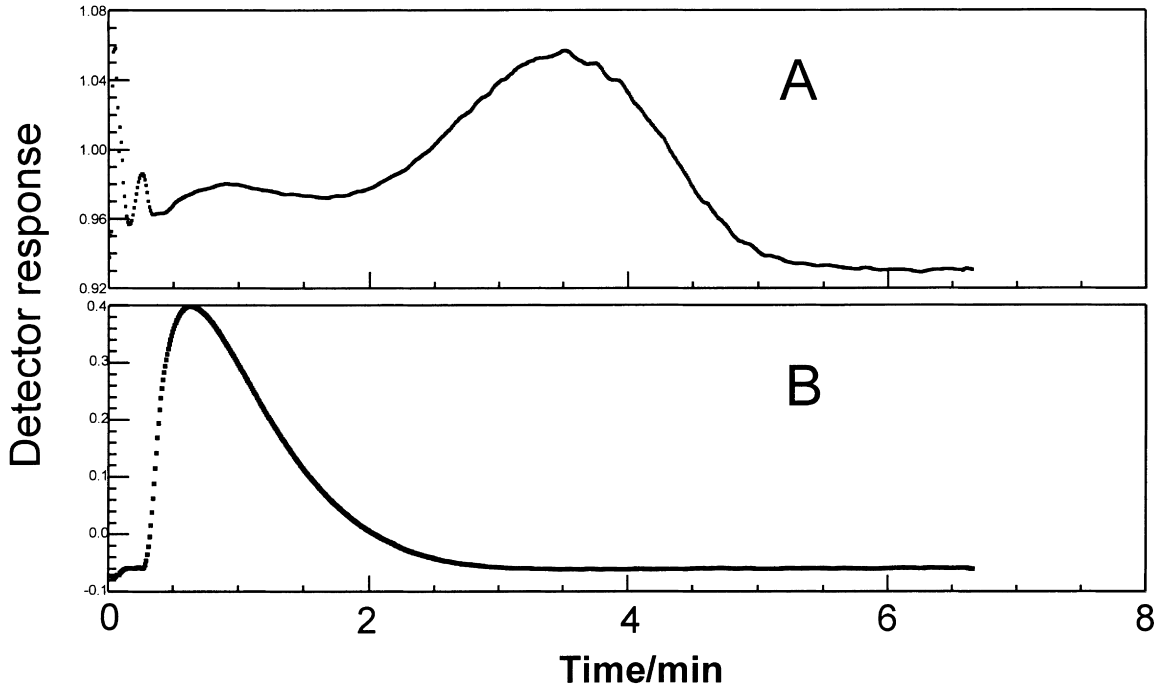

Fig. 7. The responses from the MALS detector (A) (90° signal) and the refractive index detector (B) for HPMC 50. Carrier: 10% methanol/90% 10 mM NaCl. Conditions: Inlet flow rate V_{in} 1.5 ml/min; crossflow rate $V_c = 0.47$ ml/min; $V_c/V_{out} = 0.46$; $t^0 = 0.31$ min.

changes are relatively small and could to some extent be explained by uncertainties in the experiments. The second virial coefficient A_2 decreased for the two high molar mass samples whereas an increase is observed for HPMC 50 (Table 2). Thus, the decrease in methanol content affected the samples differently. This means that methanol should be a more favourable solvent than the aqueous salt solution for HPMC 4000 and especially HPMC 10000 whereas the opposite holds for HPMC 50.

Furthermore, for HPMC 50, a bimodal shape of the MALS signal was observed with flow FFF-MALS in this medium (Fig. 7). This bimodality was only seen at very low cross flow rates and was smeared out when the retention was increased. This stresses the necessity to vary the flow rates in order to maximise the reliability of the distributions. The second peak, which completely dominates the MALS fractogram, is not at all seen in the refractometer signal. This indicates that there is a very small population that reaches large sizes, which may be interpreted as polymer aggregates although this is contradictory to the good solvent contact predicted by the high A_2-values. Another possible explanation is that impurities, having a compact structure

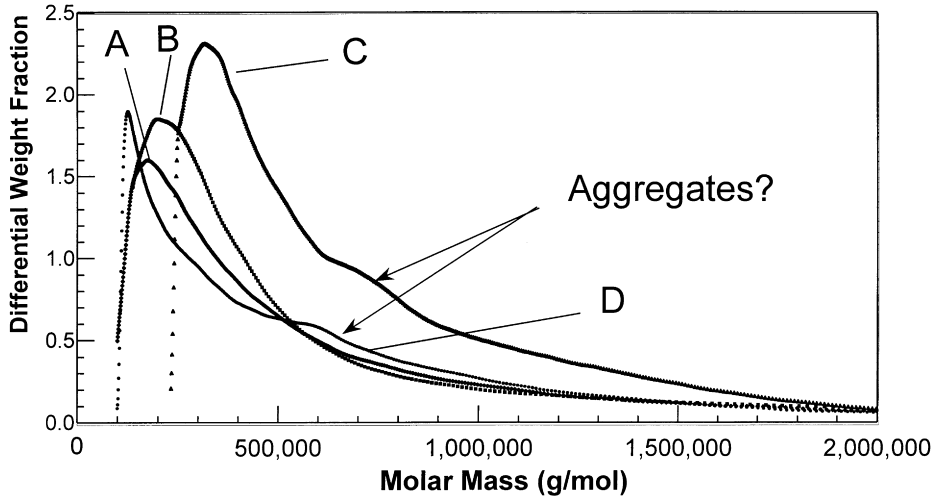

Fig. 8. The molar mass distribution for HPMC 10000 obtained in four different solvents: (A) 50% methanol/50% 10 mM NaCl; (B) 10% methanol/90% 10 mM NaCl; (C) 1 mM NaCl; and (D) 100 mM NaCl.

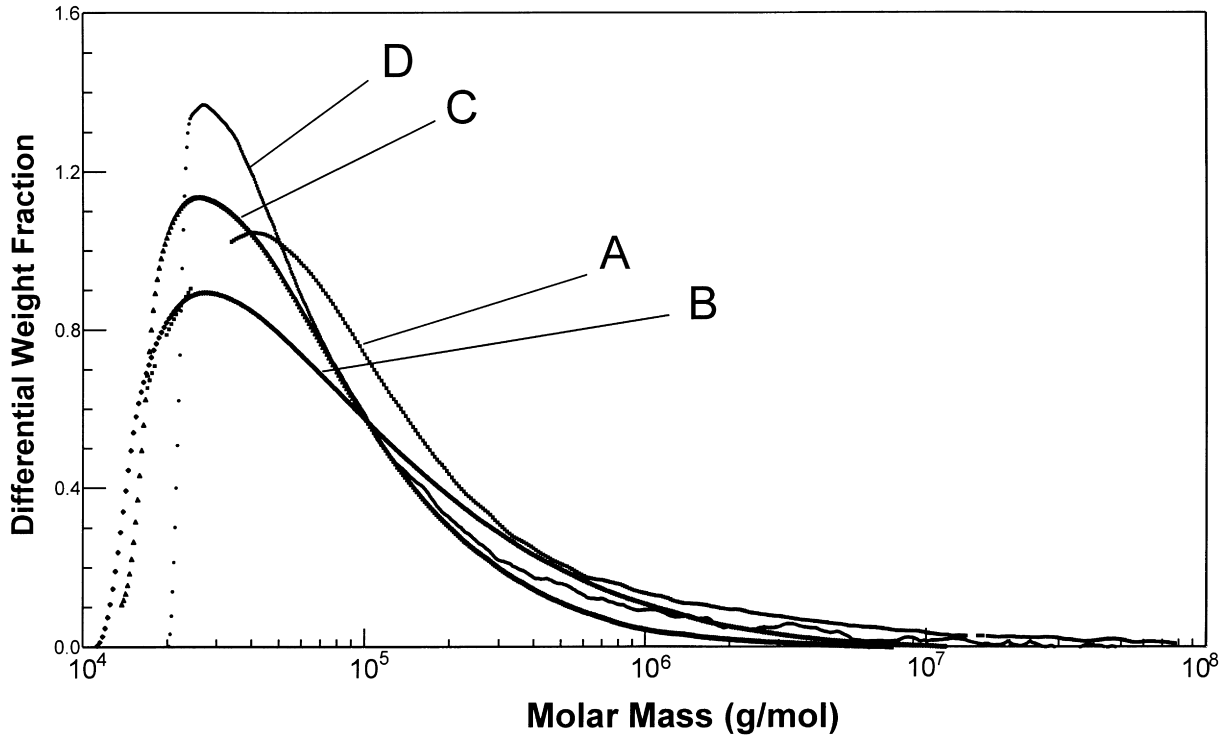

Fig. 9. The molar mass distribution for HPMC 50 obtained in four different solvents: (A) 50% methanol/50% 10 mM NaCl; (B) 10% methanol/90% 10 mM NaCl; (C) 1 mM NaCl; and (D) 100 mM NaCl.

and thus giving a large MALS response, could be present in the sample. Similar phenomenon has been observed previously for modified celluloses (Porsch, Nilsson & Sundelöf, 1997). The presence of large material may further explain the differences seen in the M_w and the M_w/r_{Gz}-ratio for the two methods. The averages obtained from MB-MALS are more easily affected by presence of large, highly scattering components than the averages estimated from the combined separation-light scattering method, especially when the number of large components is very small such in this case. If these components are unrelated to the polymer, e.g. impurities, it will lead to an overestimation of the M_w from MB-MALS. However, the differences between the methods observed here are too small to be used for further conclusions concerning this possible artifact for MB-MALS. Using proper flow conditions, flow FFF-MALS is, in this case, a more efficient instrument for detecting large sample components.

3.2. Salt–water mixtures

The three HPMCs were studied also in salt/water mixtures without any methanol present. The carriers used were NaCl solutions of two different ionic strengths, namely 1 and 100 mM. As expected, the HPMC samples show a different behaviour in these methanol-free solutions. In the 1 mM NaCl solution, the obtained molar masses were substantially higher than in the previously examined methanol mixtures. This increase in M_w was detected by both methods. For HPMC 10000, the obtained M_w was almost doubled to over 630,000 and the r_{Gz} was close to 90 nm according to flow FFF-MALS (Table 3). The M_w/r_{Gz}-ratio has increased which indicates a formation of more compact structures. However, the polydispersity index, M_w/M_n, remained unchanged despite the increase in M_w. The molar mass distribution for HPMC 10000 is shown in Fig. 8. It is clear that there is a shift towards higher molar mass. The distribution is rather abruptly interrupted at 200,000 g/mol, indicating a poor separation efficiency of the small material which may explain the low observed polydispersity. Attempts to increase the retention and thus the resolution of the low part of the distribution by increased crossflow resulted in reduced recoveries. Generally, the recovery was significantly lower than in the methanol carriers, which contributes to the difficulty in obtaining consistent results for complete distribution in this particular solvent.

A higher molar mass was also observed for HPMC 4000, where a 70% increase in M_w to 450,000 was obtained (Table 3). The radius of gyration was 84 nm leading to an increased M_w/r_{Gz}-ratio also for this sample. The MB-MALS measurements confirm this result but gave a lower r_G for HPMC 4000, 69 nm, indicating an even more compact conformation. This changes in molar mass and conformation observed for HPMC 4000 and 10000 were not seen at all for HPMC 50. For this sample, the molar mass values were in principle the same as obtained in the methanol mixtures. The radius of gyration, however, clearly increased as seen

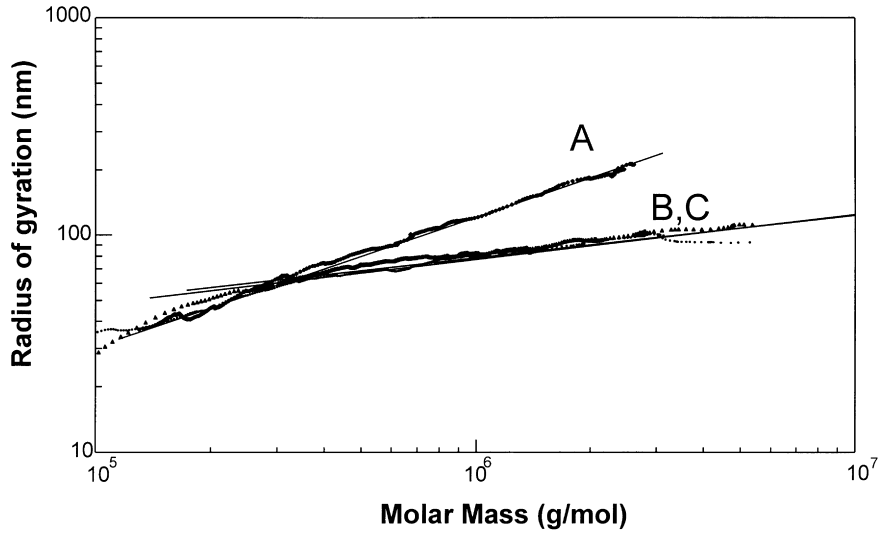

Fig. 10. The logarithm of the radius of gyration plotted versus the logarithm of the molar mass for HPMC 10000 in three different solvents: curve (A) 50% methanol/50% 10 mM NaCl; curve (B) 1 mM NaCl; and curve (C) 100 mM NaCl. The slopes of curve A, B and C are 0.58, 0.32 and 0.29, respectively.

with both methods although the previous observation that flow FFF-MALS provides larger r_{Gz}-values than MB-MALS also holds for this solvent. The increased r_{Gz} and unchanged M_w leads to a reduced M_w/r_{Gz}-ratio which is the opposite to the case with HPMC 4000 and HPMC 10000. It seems reasonable that HPMC 50 should be affected by the solvent in a similar way to the other two HPMCs. However, the A_2 term also changes differently for the three samples. It is somewhat increased for HPMC 50 in the pure 1 mM NaCl salt solution while it is decreased for HPMC 4000 and HPMC 10000. Thus, the solution behaviour for these samples is not identical which probably reflects the difference in their origin. It is therefore difficult to interpret the difference in results from the two methods.

When the ionic strength was increased to 100 mM, the observed molar mass was reduced for all three samples. For HPMC 4000 and HPMC 10000, the M_w obtained was still a bit higher than observed in the methanol mixtures. For HPMC 50, the radius of gyration was increased further leading to a decreased M_w/r_{Gz}-ratio. A similar decrease was also detected for HPMC 4000 and 10000 indicating a better solvent which is supported by the higher A_2 values seen for all three samples.

4. Discussion

The aim of this work was to study changes in size and molar mass caused by different compositions of the solvent. According to the results obtained, these parameters do change but in different directions depending on the HPMC-sample analysed. The molar mass distributions of HPMC 10000 and HPMC 50 in the different solvents are seen in Figs. 8 and 9. For HPMC 10000, the molar mass distribution shifts towards higher values when methanol is excluded from the solvent. There is also an indication of a bimodal distribution in the salt solutions for HPMC 10000, which suggests an increased presence of aggregates. This seems possible according to the decreased A_2-values observed in the methanol-free solvents. The 1 mM NaCl solution gave the highest molar mass and also the M_w/r_{Gz}-ratio (Tables 2 and 3) reaches its maximum here indicating a compact conformation. This is further supported in the so-called conformation plot (Wyatt, 1993) (Fig. 10), i.e. the log r_G vs. log M_w plot, where the slope gives conformational information. The slope of curve A (50% methanol mixture) is 0.6, indicating an expanded conformation, whereas the curves corresponding to the methanol-free solvents have a slope below 0.3, suggesting very compact structures. Although a value below 0.3 seems unreasonably low for a linear polymer and an experimental artefact therefore cannot be excluded (Wittgren, Borgström, Wahlund & Piculell, 1998), the result together with the increased M_w/r_{Gz}-ratio clearly illustrates a more compact structure due to the change in solvent. HPMC 4000 behaves in a similar way to HPMC 10000.

For HPMC 50 however, the picture is different. The molar mass increases as the methanol content increases but still, HPMC 50 is less influenced by the methanol content than is HPMC 10000. The difference in molar mass distributions obtained in the various solvents is less pronounced (Fig. 9). According to the A_2-values, HPMC 50 has a more favourable polymer–solvent interaction in all four solvents compared to the high molar mass samples. Thus, it is the high molar mass HPMCs that are mostly affected by changes in the solvent compositions. In addition, aggregates of the high molar mass celluloses may be of such a large size that they are practically immobilised in the flow FFF channel and therefore not detected. This is, as mentioned previously, often related to too high crossflows in the separation channel, which would further contribute to the low recovery observed in the methanol-free solvents. The

MB-MALS measurements, where the sample is unaffected of any separation process that might alter the sample composition, provided also higher molar mass values for HPMC 4000 and HPMC 10000 than flow FFF-MALS. This is another indication that aggregates could be present but not explicitly detected by flow FFF-MALS.

According to both methods, the Shin-Etsu made HPMC 50 and the two DOW products HPMC 4000 and HPMC 10000 respond differently to changes in the solvent compositions. According to the observations summarised above, HPMC 50 seems to be more lyophilic than the other two polymers. In the literature, methanol/water mixtures are mentioned as being especially favourable for modified celluloses but the solution mechanism is little understood. For example, Porsch et al. (1997) suggests that a more hydrophilic substituted cellulose, absorbing more water, may even form associates in methanol/water mixtures in order to share a more hydrophilic environment. This may be one explanation to the proposed aggregation observed for HPMC 50 in the 10% methanol mixture. However, in this study the increased solvent–polymer contact predicted for methanol/water mixtures is best illustrated for the high molar mass HPMCs. Another possible explanation to the observed aggregation may be presence of unsubstituted regions along the cellulose chain that have crystalline properties (Lindman & Thuresson, 1999). Such regions would be strongly associated and insoluble in aqueous solutions. It is not unlikely that the HPMC samples studied here contain this inhomogeneity to different extents since the substitution pattern is an effect of the manufacturing process.

The use of two different methods for the characterisation of such a complex polymer as HPMC increases the possibility of creating a complete picture of the size-related properties and differences between commercially produced. MB-MALS turns out to be especially valuable for studies of solvent effects where the determination of the second virial coefficient directly may resolve differences in quality between different polymers. When properly conducted, it can thus serve as a fast and easy check of molar mass and size averages, as well as the quality of the solvent. However, the combination of a separation technique, such as flow FFF, and MALS is generally the more powerful option since distributions of mass and size can also be obtained where changes in solution behaviour such as aggregation, chain expansion or contraction are more easily spotted.

Acknowledgements

This study was supported by grants from the Swedish Research Council for Engineering Sciences. The development of the flow FFF system was made possible by grants from the AstraZeneca R&D Mölndal, the Carl Trygger Foundation and the Crafoord Foundation. Dr Stefan Nilsson, Dr Bedrich Porsch and Professor Lars-Olof Sundelöf, Uppsala University, are gratefully acknowledged for their comments on this work in progress.

References

Adolphi, U., & Kulicke, W. -M. (1997). Coil dimensions and conformation of macromolecules in aqueous media from flow field-flow fractionation/multi-angle laser light scattering illustrated by studies on pullulan. *Polymer, 38*, 1513–1519.

Giddings, J. C. (1973). The conceptual basis of field-flow fractionation. *Journal of Chemical Education, 1*, 123–125.

Giddings, J. C. (1993). Field-flow fractionation: analysis of macromolecular, colloidal, and particulate materials. *Science, 260*, 1456–1465.

Harding, S. E., Varum, K. M., Stokke, B. T., & Smidsrod, O. (1991). Molecular weight determination of polysaccharides. *Advances in Carbohydrate Analysis, 1*, 63–104.

Kratochvil, P. (1987). In A. D. Jenkins, Classical light scattering from polymer solutions. *Polymer Science Library, 5*. Amsterdam: Elsevier.

Lindman, B., & Thuresson, K. (1999). Association in non-ionic cellulose ether solutions due to microcrystallite. *Colloids and Surfaces*, 000.

Litzén, A. (1993). Separation speed, retention and dispersion in asymmetrical flow field-flow fractionation as functions of channel dimensions and flow rates. *Analytical Chemistry, 65*, 461–470.

Litzén, A., & Wahlund, K. -G. (1991). Zone broadening and dilution in rectangular and trapezoidal asymmetrical flow field-flow fractionation channels. *Analytical Chemistry, 63*, 1001–1007.

Nilsson, S., Sundelöf, L. -O., & Porsch, B. (1995). On the characterization principles of some technical important water soluble non-ionic cellulose derivatives. *Carbohydrate Polymers, 28*, 265–275.

Porsch, B., Nilsson, S., & Sundelöf, L. -O. (1997). Association of ethyl-(hydroxyethyl)cellulose solutions. *Macromolecules, 30*, 4626–4632.

Roessner, D., & Kulicke, W. -M. (1994). On-line coupling of flow field-flow fractionation and multi-angle laser light scattering. *Journal of Chromatography A, 687*, 249–258.

Wahlund, K. -G., & Giddings, J. C. (1987). Properties of an asymmetrical flow field-flow fractionation channel having one permeable wall. *Analytical Chemistry, 59*, 1332–1339.

Wittgren, B., & Wahlund, K. -G. (1997). Fast molar mass and size characterization of polysaccharides using asymmetrical flow field-flow fractionation-multi-angle light scattering. *Journal of Chromatography A, 760*, 205–218.

Wittgren, B., & Wahlund, K. -G. (1997). Effects of flowrates and sample concentration on the molar mass characterisation of modified celluloses using asymmetrical flow field-flow fractionation-multi-angle light scattering. *Journal of Chromatography A, 791*, 135–149.

Wittgren, B., Wahlund, K. -G., Derand, H., & Wesslén, B. (1996). Aggregation behaviour of an amphiphilic graft copolymer in aqueous medium studied by asymmetrical flow field-flow fractionation. *Macromolecules, 29*, 268–276.

Wittgren, B., Borgström, J., Wahlund, K. -G., & Piculell, L. (1998). Conformational change and aggregation of κ-carrageenan studied by flow field-flow fractionation and multi-angle light scattering. *Biopolymers, 45*, 85–96.

Wyatt, P. J. (1993). Light scattering and the absolute characterization of macromolecules. *Analytica Chimica Acta, 272*, 1–40.

Zimm, B. H. (1945). Molecular theory of the scattering of light in fluids. *Journal of Chemical Physics, 13*, 141.